



ELSEVIER

Contents lists available at ScienceDirect

Journal of Luminescence

journal homepage: www.elsevier.com/locate/jlumin

Energy transfer processes in Eu^{3+} doped nanocrystalline La_2TeO_6 phosphor

J. Llanos ^{a,*}, R. Castillo ^a, I.R. Martín ^{b,d}, L.L. Martín ^{a,b,c,d}, P. Haro-González ^b,
J. González-Platas ^c

^a Departamento de Química, Universidad Católica del Norte, Casilla 1280, Antofagasta, Chile

^b Departamento de Física Fundamental, Experimental, Electrónica y Sistemas, Universidad de La Laguna, 38206 La Laguna, Tenerife, Spain

^c Departamento de Física Fundamental II, Universidad de La Laguna, 38206 La Laguna, Tenerife, Spain

^d Malta Consolider Team, Santander, Spain

ARTICLE INFO

Article history:

Received 6 March 2013

Received in revised form

19 June 2013

Accepted 2 August 2013

Available online 25 August 2013

Keywords:

Inorganic materials

Optical materials

Sol–gel process

Luminescence

Rare-earth compounds

ABSTRACT

La_2TeO_6 nanocrystals doped with Eu^{3+} ions have been prepared by the Pechini sol–gel process. A total of seven samples obtained with different Eu^{3+} concentrations (1–7%). The Eu^{3+} ions are usually taken as probe ions to test the local structure of the lanthanide in solids. Analyzing the luminescence has been shown two different sites for the Eu^{3+} ions (in good agreement with the crystallographic analysis). Moreover, the luminescence properties have been analyzed as function of the Eu^{3+} doping concentration in order to study the interaction between these ions. Under direct excitation into the $^5\text{D}_0$ level (at 578 nm) the corresponding decay curves show a pure exponential character independently of the Eu^{3+} concentration. However, the decay curves obtained for the $^5\text{D}_1$ level becomes non-exponential for the higher doped nanocrystals samples indicating that the energy transfer processes are important.

© 2013 Elsevier B.V. All rights reserved.

1. Introduction

Inorganic compounds doped with europium are one of the most important phosphors since they were proposed as phosphors to be used on the cathodic ray tubes of color televisions [1]. By the other hand, in the last decade the Eu^{3+} -doped inorganic phosphors have attracted considerable interest due to their use as red-emitting phosphors in solid-state lighting devices (SSL) [2–8]. In particular, materials such as tungstate, vanadate, oxynitrides, silicates, etc. have extensively studied in order to obtain new red-emitting phosphors for solid state lighting devices based on InGaN LEDs [9–13].

Recently, Wenzl et al. reported about the approach to improve the quality of phosphors for use in the fabrication of white LED [14]. Another important factor that affects the emission of the Eu^{3+} is the environment of the activator in the matrix. The knowledge of the site distribution of the cations Eu^{3+} on the host structure is also an important factor when the luminescent properties of the phosphor are analyzed [15].

The emission of the Eu^{3+} around 590–600 nm is due to the magnetic dipole transition $^5\text{D}_0 \rightarrow ^7\text{F}_1$, this transition is insensitive to the symmetric environment of the rare-earth ion, whereas the emission around 610–620 nm is due to the electric dipole $^5\text{D}_0 \rightarrow ^7\text{F}_2$, which is

highly sensitive to the symmetry of the Eu^{3+} cation, indicates that Eu^{3+} occupies a non-centrosymmetric site [16].

The energy transfer process between Eu^{3+} ions is an important factor influencing the phosphor characteristics of different materials. These processes could depopulate a level and in this way change the emission spectra as function of the Eu^{3+} concentration. In this way, the chromaticity coordinates defined by the International Commission on Illumination (CIE) could be affected.

In the last few years, we have been actively involved in the preparation and characterization of red-emitting phosphors. We have prepared the Eu^{3+} , and the $\text{Eu}^{3+}:\text{Gd}^{3+}$ -doped orthotellurates, Ln_2TeO_6 ($\text{Ln}=\text{La}, \text{Gd}$) as nanostructured materials. We have chosen, La_2TeO_6 as a host structure for the phosphors because its chemical and thermal stability [17–19].

In this paper, we have been carried out a detailed analysis of the energy transfer processes between the luminescent excited levels ($^5\text{D}_1$ and $^5\text{D}_0$) of Eu^{3+} ions as function of the concentration. The lifetimes of the Eu^{3+} doped compounds as function of activator ions concentration were re-investigated using tunable dye laser. The site-occupancy of Eu^{3+} in $\text{La}_{2-x}\text{Eu}_x\text{TeO}_6$ was also investigated.

2. Experimental

All the $\text{La}_{2-x}\text{Eu}_x\text{TeO}_6$ samples in this study were prepared by the Pechini sol–gel process [20]. According to the stoichiometric formula, 4.36×10^{-3} mol of La_2O_3 (Aldrich, 99.99% pure) and

* Corresponding author. Tel.: +565 535 5624; fax: +565 535 5632.

E-mail address: jllanos@ucn.cl (J. Llanos).

Eu_2O_3 (Aldrich, 99.99% pure) in different ratios were dissolved in 30 ml de HNO_3 (0.5 M) under vigorous stirring. The pH of the solution was adjusted between 1 and 2. When the oxides were completely dissolved, they were mixed with water–ethanol ($v/v=1:7$) solution containing citric acid (Merck, A.R.) as chelating agent for the metal ions and 4.36×10^{-3} mol of H_6TeO_6 (Aldrich, 97.5–102.5% pure). The molar ratio of telluric acid to citric acid was 1:2. Afterward, ca. 1.25 g de polyethylene glycol (PEG, M.W.=20,000, Fluka, A.R.) was added as cross-linking agent. Transparent sols were obtained after stirring for 2 h. The sols were dried in a 346 K water bath. When the sols were completely dry, they were annealed at 643 K in a furnace. After annealing, the resulting powders were fired to 1073 K with a heating rate of 1 K/min and kept there for 2 h. Optical inspection of the products showed homogeneous powders of white colors.

To verify the purity of the phase, powder X-ray diffraction (PXRD) patterns were collected with a Bruker AXS D8 Advance diffractometer in the 2θ range from 10° to 60° , with $\text{CuK}\alpha$ radiation ($\lambda=0.15045$ nm) operated at 40 kV and 30 mA. All measurements were carried out at room temperature.

Broad band emission spectra were obtained by exciting the samples with light from a 250 W incandescent lamp passed through a 0.25 m single-grating monochromator. Fluorescence was detected through a 0.25 m double-grating monochromator with a photomultiplier. For laser-excited site selective spectra a tuneable dye laser operating with Rhodamine 6G, pumped by a Q-switched 532 nm frequency-doubled Nd–YAG laser, was used. The spectral line-width was 0.15 cm^{-1} and the pulse width 5 ns. A helium continuous flow cryostat was used for measurements in the range from 13 to 290 K. The temporal decays curves were acquired by an oscilloscope controlled by a personal computer.

3. Results and discussion

A total of seven compositions were synthesized in the system $\text{La}_{2-x}\text{Eu}_x\text{TeO}_6$ ($x=0.02, 0.04, 0.06, 0.08, 0.10, 0.12, 0.14$). The powder X-ray diffraction patterns of the compounds reveal that all the samples crystallized isostructurally with the orthorhombic La_2TeO_6 -type structure in the space group $P2_12_12_1$ [21]. The powder X-ray diffraction patterns of the all samples are shown in Fig. 1.

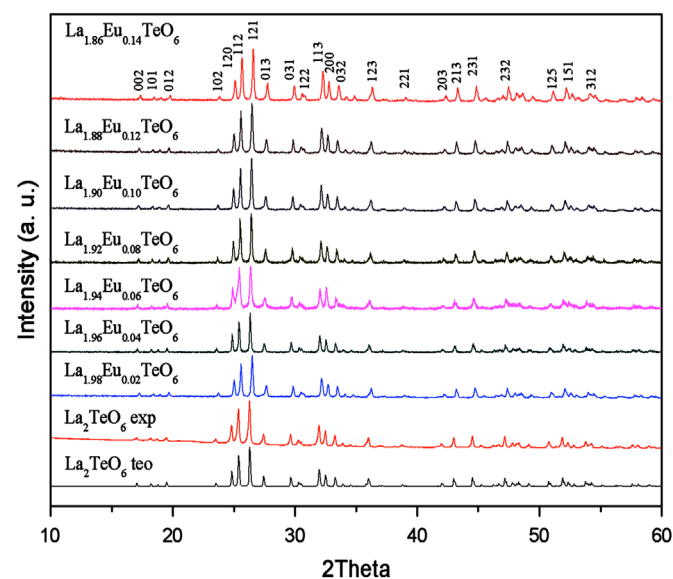


Fig. 1. XRD patterns of $\text{La}_{2-x}\text{Eu}_x\text{TeO}_6$ ($x=0.02, 0.04, 0.06, 0.08, 0.10, 0.12, 0.14$).

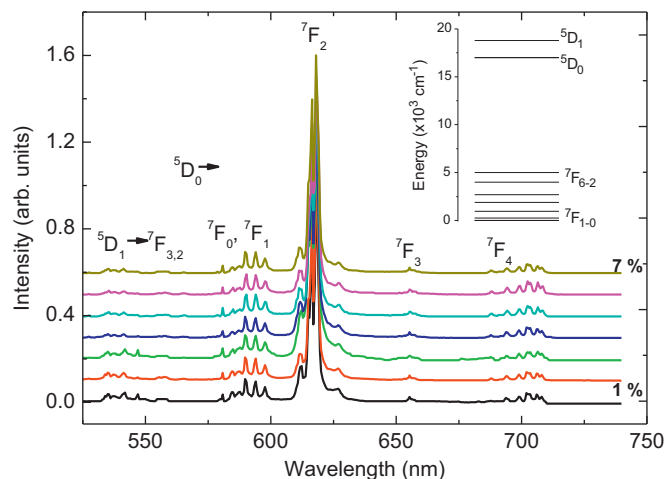


Fig. 2. Emission spectra obtained in $\text{La}_{2-x}\text{Eu}_x\text{TeO}_6$ ($x=0.02, 0.04, 0.06, 0.08, 0.10, 0.12, 0.14$) nanocrystals. The inset shows a partial energy level diagram of Eu^{3+} ions.

In the Fig. 2 are shown the emission spectra obtained at RT exciting at 400 nm for the different doped samples. As can be seen, all the spectra are very similar and they show well-resolved peaks indicating that the Eu^{3+} ions, in good agreement with the X-ray diffraction patterns, are well incorporated into the structure of the nanocrystals. The intra-configurational 4f–4f transitions of the Eu^{3+} ions were identified comparing the peak energies with the free Eu^{3+} ion energy level diagram (see inset of Fig. 1). The observed emission bands clearly show a structure due to the splitting of the $7F_J$ ($J=1-4$) levels induced by the crystal-field. However, for the electronic transition between the non-degenerate $5D_0$ and $7F_0$ levels, at about 578 nm, a single line is expected because this transition cannot be splitted by any local point symmetry around the Eu^{3+} ion.

When the Eu^{3+} doped samples are excited in close proximity to 578 nm some changes are observed in the emission spectra. In order to analyze if these changes are due to different sites occupied by the Eu^{3+} ions have been carried out excitation spectra at 13 K and RT. As example, the results obtained for the sample doped with 4% are shown in Fig. 3, where two different sites are clearly observed for the Eu^{3+} ions. The excitation bands are located about 577.5 nm and 579.5 nm at RT. Moreover, when emission spectra have been obtained under excitation to these wavelengths different emission spectra have been found (Fig. 4). All these results, confirm that the Eu^{3+} ions are located in two non-equivalent sites. According to the crystal structure of the La_2TeO_6 nanocrystals, it is expected that the Eu^{3+} substitute to the La^{3+} ions. Two different sites for the lanthanide anions are in host lattice, both coordination spheres are shown in Fig. 5. The local symmetry for the two different crystallographic sites is C_1 , this lack of an inversion center in both polyhedra is in good agreement with the emission spectra obtained for $\text{La}_{2-x}\text{Eu}_x\text{TeO}_6$ compounds. It is possible to observe two different luminescent intensities in the emission spectra because of the two different crystallographic sites (both in the 4a position), one of them possesses an inferior symmetry, and in other words some distances Eu–O are not only longer, but also the coordination polyhedron is more distorted, these conditions are involved in the chromaticity of the two luminescent centers.

Although there is an important spectroscopy difference for the Eu^{3+} sites in the nanocrystals, the decay curves for the $5D_0$ level obtained at room temperature by exciting around 578 nm and detecting about 620 nm are very similar for all the doped samples and the two sites (Fig. 4). Respect to the $5D_1$ level, the decay curves

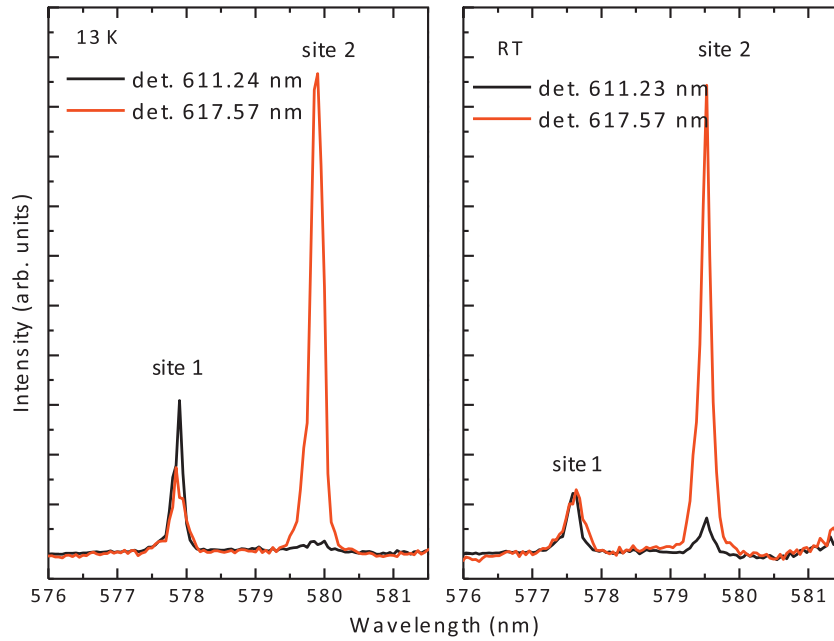


Fig. 3. Excitation spectra obtained at 13 K and RT of $\text{La}_{1.92}\text{Eu}_{0.08}\text{TeO}_6$ nanocrystals. Two different sites are clearly resolved.

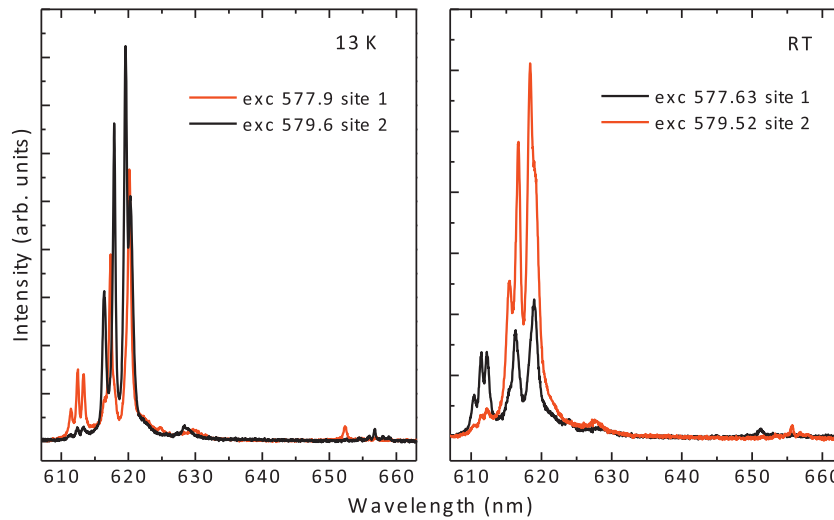


Fig. 4. Emission spectra obtained at 13 K and RT of $\text{La}_{1.92}\text{Eu}_{0.08}\text{TeO}_6$ nanocrystals.

of the fluorescence from this level have been obtained by exciting at room temperature the ${}^7\text{F}_1 \rightarrow {}^5\text{D}_1$ transition at 532 nm and monitoring the ${}^5\text{D}_1 \rightarrow {}^7\text{F}_2$ emission at 551 nm. These curves are non-exponential indicating that the energy transfer processes are relevant when concentration increases (Fig. 6). This energy transfer process can be due to the following cross relaxation channel



This energy transfer process can also be verified in the emission spectra shown in Fig. 3. As can be seen in this figure, when the Eu^{3+} concentration is increased the emission coming from the ${}^5\text{D}_1$ level is lowered respect to the emission bands coming from the ${}^5\text{D}_0$ level. This result is a consequence of the mechanism described by Eq. (1).

In order to analyze the dynamic of the ${}^5\text{D}_1$ decay curves, the Inokuti–Hirayama model [22] has been used. In this model, it is assumed that the activator ions are randomly distributed in the

host structure and are excited by a pulsed excitation. Therefore, assuming a dipole–dipole character for the interaction between donor and acceptor ions, the temporal evolution of the ions excited to the ${}^5\text{D}_1$ level (donors) could be described by

$$I_D(t) = I_D(0)e^{-t/\tau_D - Q[t/\tau_D]^{1/2}} \quad (2)$$

where τ_D is intrinsic lifetime of this level and Q is given by

$$Q = \frac{4\pi}{3}\pi^{1/2}C_A(C_{DA}\tau_D)^{1/2} \quad (3)$$

where C_A is the Eu^{3+} concentration and C_{DA} is the donor–acceptor energy transfer parameter. A good fitting to the decay curves is obtained with this model, assuming the same value for the intrinsic lifetime τ_D (about 67 μs), the values for the energy transfer Q are 0.39, 0.53, 0.92, 1.05, 1.18, 1.47 and 1.68 $\mu\text{s}^{-1/2}$, for the seven samples studied to 1% to 7% of Eu^{3+} , respectively (see Fig. 7). As can be seen, the increase observed in the Q value is

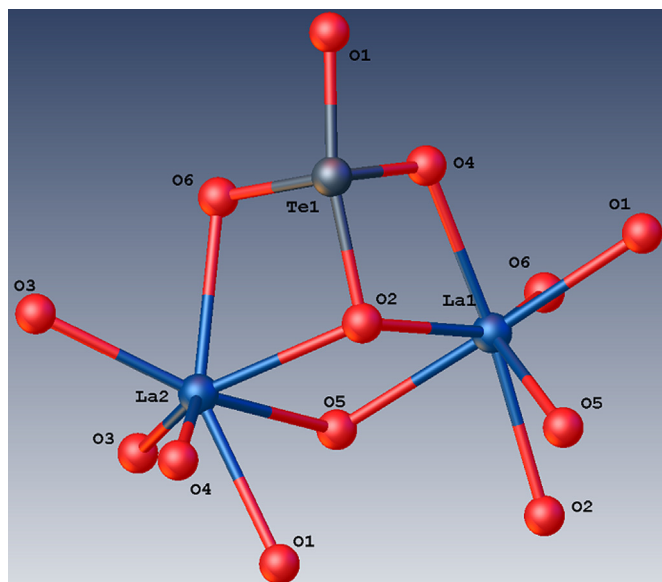


Fig. 5. Scheme of the La_2TeO_6 structure indicating two different sites for the lanthanide ions.

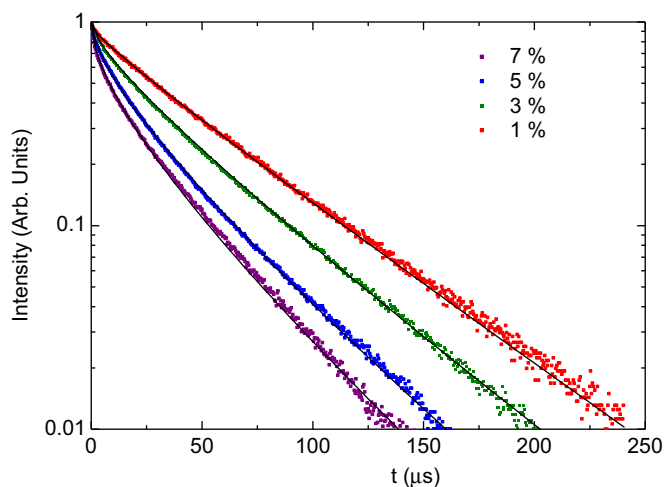


Fig. 6. Lifetime of Eu^{3+} as a function of its concentration.

nearly proportional to the Eu^{3+} concentration, as predicted by Eq. (3). According to the Inokuti–Hirayama model, these results indicate that Eu^{3+} ions are localized randomly in the host crystal structure and rules out the possibilities of forming clusters.

4. Conclusions

Using laser spectroscopy have been found two different sites for the Eu^{3+} ions in the La_2TeO_6 nanocrystals. Moreover, the energy transfer parameter (Q) for the luminescent level $^5\text{D}_1$ is proportional to the Eu^{3+} concentration. This result confirms that there are not clusters of Eu^{3+} ions in the La_2TeO_6 nanocrystals.

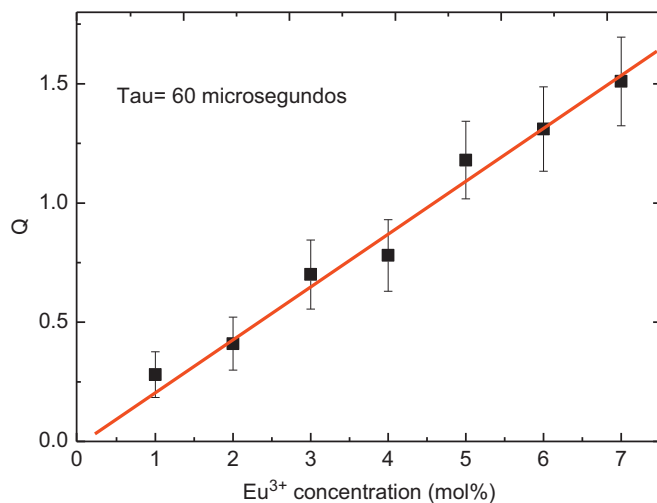


Fig. 7. Dependence of the energy transfer parameter Q with the Eu^{3+} concentration.

Acknowledgments

The authors are grateful to Fondecyt 1090327, Comisión Interministerial de Ciencia y Tecnología (MAT2010-21270-C04-02), Malta Consolider Ingenio 2010 (CSD2007-0045) and FPI of Gobierno de Canarias for financial support.

References

- [1] A.K. Levine, F.C. Palilla, *Trans. N.Y. Acad. Sci.* 27 (1965) 517.
- [2] R. Mueller-Mach, G. Mueller, M.R. Krames, H.A. Hoppe, F. Stadler, W. Schnick, T. Juestel, P. Schmidt, *Phys. Status Solidi A* 202 (2005) 1727.
- [3] S. Neeraj, N. Kijima, A.K. Cheetham, *Solid State Commun.* 131 (2004) 65.
- [4] Y.-F. Liu, Z.-P. Yang, Q.-M. Yu, *J. Alloys Compd.* 509 (2011) L199.
- [5] L. Zhou, J. Huang, F. Gong, Y. Lan, Z. Tong, J. Sun, *J. Alloys Compd.* 495 (2010) 268.
- [6] H.A. Höpfe, *Angew. Chem. Int. Ed.* 48 (2009) 3572.
- [7] J. Llanos, R. Castillo, *J. Lumin.* 130 (2010) 1124.
- [8] C.C. Mi, Z.H. Tian, B. Han, C. Mao, S. Xu, *J. Alloys Compd.* 525 (2012) 154.
- [9] P.F.S. Pereira, A.P. de Moura, I.C. Nogueira, M.V.S. Lima, E. Longo, P.C. de Sousa Filho, O.A. Serra, E.J. Nassar, I.L.V. Rosa, *J. Alloys Compd.* 526 (2012) 149.
- [10] S. Tang, M. Huang, J. Wang, F. Yu, G. Shang, J. Wu, *J. Alloys Compd.* 513 (2012) 474.
- [11] P. Alemany, I.de P.R. Moreira, R. Castillo, J. Llanos, *J. Alloys Compd.* 513 (2012) 630.
- [12] F.A. Sigoli, M.R. Davalos, M. Jafelicci Jr., *J. Alloys Compd.* 334 (2002) 308.
- [13] X. Zhang, M. Gong, *J. Alloys Compd.* 509 (2011) 2850.
- [14] C. Sommer, P. Hartmann, P. Pachler, H. Hoschopf, F.P. Wenzl, *J. Alloys Compd.* 520 (2012) 146.
- [15] Ch. Qin, Y. Huang, H.J. Seo, *J. Alloys Compd.* 534 (2012) 86.
- [16] S. Shinoya, W.M. Yen (Eds.), *Phosphor Handbook*, CRC Press, Boca Raton, FL, 1998.
- [17] J. Llanos, R. Castillo, W. Alvarez, *Mater. Lett.* 62 (2008) 3597.
- [18] R. Castillo, J. Llanos, *J. Lumin.* 129 (2009) 465.
- [19] J. Llanos, R. Castillo, D. Barrionuevo, D. Espinoza, S. Conejeros, *J. Alloys Compd.* 485 (2009) 565.
- [20] M.P. Pechini, U.S. Patent 3330697, 1967.
- [21] S.F. Meier, T. Schleid, *J. Solid State Chem.* 171 (2003) 408.
- [22] M. Inokuti, F.J. Hirayama, *J. Chem. Phys.* 43 (1965) 1978.